


Comparative Analysis of Transcriptional Profile Changes in Larval Zebrafish Exposed to Zinc Oxide Nanoparticles and Zinc Sulfate

Ryeo-Ok Kim¹ · Jin Soo Choi² · Byoung-Chul Kim¹ · Woo-Keun Kim¹ 

Received: 8 July 2016 / Accepted: 29 November 2016 / Published online: 19 December 2016
© Springer Science+Business Media New York 2016

Abstract Many studies of the toxic effects of zinc oxide nanoparticles (ZnO NPs) in aquatic organisms have been performed because of increasing ZnO NP use. However, the toxicological pathways are not understood. In this study, ZnO NPs were found to be more toxic than ZnSO₄ to zebrafish larvae, but ZnO NP toxicity did not involve transcript alterations. Biological processes affected by ZnO NPs and ZnSO₄ were investigated by performing ingenuity pathway analysis on differently expressed genes in larvae exposed to sub-lethal ZnO NP and ZnSO₄ concentrations. We identified upregulated and downregulated differently expressed genes in fish exposed to ZnO NPs and ZnSO₄, and found that ZnO NPs slightly induced cell differentiation and pathways associated with the immune system and activated several key genes involved in cancer cell signaling. The results may be key to predicting and elucidating the mechanisms involved in ZnO NP and ZnSO₄ toxicity in zebrafish larvae.

Keywords Zebrafish · Zinc oxide nanoparticles · Microarray · Ingenuity pathway analysis

Zinc oxide (ZnO) nanoparticles (NPs) are widely used in various commercial and industrial products, such as batteries, cement, ceramics, fire retardants, foods, glass, paints, pigments, plastics, and rubber (Aitken et al. 2006; Chen

et al. 2014). It has been estimated that between 550 and 33,400 tonnes of ZnO NPs are produced each year worldwide. The global production volume of ZnO NPs is the third highest of the NPs that contain metals, after SiO₂ NPs and TiO₂ NPs (Bondarenko et al. 2013). Their widespread use has led to ZnO NPs being found in environmental media, and ZnO NP concentrations in sediment, sewage sludge, soil, surface water, and wastewater of 0.49–56, 13.6–64.7, 0.026–0.66, 1–60, and 0.22–1.42 µg/L, respectively, have been predicted and/or measured (Gottschalk et al. 2009, 2010). Higher ZnO NP concentrations have been found in aquatic environments that are the final destinations of contaminants than in other environments (Bystrzejewska-Piotrowska et al. 2009).

The dose is not the only factor that is used to evaluate the toxicities of NPs unlike for conventional contaminants. The physicochemical properties of the NPs, such as the degree to which aggregations form and the chemical compositions, particle shapes, and sizes of the NPs can affect the toxicities of the NPs. For metal-based NPs, it has been found that rod-shaped iron oxide nanoparticles are more toxic than spherical nanoparticles to murine macrophage cells, that the toxicities of silver NPs to bacillus are charge-dependent, and that amorphous TiO₂ NPs 30 nm in diameter induce reactive oxygen species more than do other TiO₂ NPs (Jiang et al. 2008; El Badawy et al. 2010; Lee et al. 2014). However, the roles the physicochemical properties of ZnO NPs play in the aquatic toxicities of the NPs have not been fully elucidated. In recent studies, the release of Zn²⁺ ions was suggested to be an important factor affecting ZnO NP toxicity (Xia et al. 2011; Fukui et al. 2012; Gilbert et al. 2012). It is therefore necessary to compare the toxicities of ZnO NPs and ZnSO₄ (an efficient source of soluble zinc ions) to gain an understanding of the contributions of other factors to the aquatic toxicities of ZnO NPs.

✉ Woo-Keun Kim
wookkim@kitox.re.kr

¹ System Toxicology Research Center, Korea Institute of Toxicology, Daejeon 34111, South Korea

² Future Environmental Research Center, Korea Institute of Toxicology, Jinju 52834, South Korea

The development of omics techniques has made it possible to simultaneously assess the expression profiles of thousands of genes in response to different stresses (Ung et al. 2010). Omics techniques can provide insights into the mechanisms involved in toxic effects and allow biomarkers related to molecular level responses to be screened rapidly (Long et al. 2012; Griffitt et al. 2013). Griffitt et al. (2013) recently found that the chronic exposure of zebrafish (*Danio rerio*) to Ag NPs caused transcriptomic changes related to cellular restructuring, developmental processes, and the repair of DNA damage. However, despite the advantages of omics techniques, only a few attempts have been made to investigate the toxicities of ZnO NPs to aquatic organisms.

The zebrafish is a small and transparent fish that is easy to maintain. Zebrafish continually reproduce, and embryogenesis is rapid (Westerfield 1995; Hill et al. 2002; Zhao et al. 2013). The zebrafish genome has been sequenced, and genetic information on zebrafish is being accumulated quickly (Berry et al. 2007). Zebrafish are commonly used as an animal model in high-throughput acute toxicity studies, and zebrafish have been used to assess the toxicities of nanomaterials (Lin et al. 2013; Felix et al. 2013). Combining a well-established model organism and a microarray platform capable of assessing changes in a large number of genes would allow detailed and accurate insights into the molecular mechanisms underlying the adaptive responses of fish to toxic substances to be gained.

The objectives of this study were: (1) to compare the toxicities of ZnO NPs and ZnSO₄ to zebrafish larvae in acute toxicity tests; (2) to identify differently expressed genes (DEGs) by performing whole gene expression profiling on larval zebrafish exposed to low and sub-lethal concentrations of ZnO NPs and ZnSO₄; and (3) to use a pathway analysis tool to attempt to identify upstream biological

causes and probable downstream effects of sub-lethal concentrations of ZnO NPs and ZnSO₄.

Materials and Methods

The uncoated ZnO NPs used in the experiments had nominal sizes of 10–30 nm, and were purchased from SkySpring Nanomaterials (Houston, TX, USA). A transmission electron microscopy image and a histogram of the size distribution of the ZnO NPs, provided by the supplier, are shown in Fig. 1. The transmission electron microscopy image was acquired using a JEM2010 instrument (JEOL, Tokyo, Japan) at 200 kV. A 100 mg/L solution of the ZnO NPs was prepared by dispersing the NPs in deionized water and sonicating the mixture at a setting of 53 W for 1 h in a Sonics instrument supplied by Sonics & Materials (Newtown, CT, USA).

The dissolved zinc in the supernatant was quantified using an inductively coupled plasma optical emission spectrometer (PerkinElmer, Waltham, MA, USA), which was equipped with an S10 autosampler (PerkinElmer). The dissolved zinc concentrations that were found are shown in Table 1.

Zebrafish larvae at 72 hpf (i.e. after hatch) were obtained from the Gyeongnam Department of Environmental Toxicology and Chemistry, Korea Institute of Toxicology. Each experiment was performed in a 250 mL beaker containing 200 mL of zebrafish culture water (carbon-filtered dechlorinated tap water), and each experiment lasted 72 h. Preliminary tests were performed to assess the toxicities of sublethal ZnO NP concentrations (0.153, 0.307, 1.228, 2.457, 4.914, 9.827, 12.284, and 122.838 μmol/L) and sublethal ZnSO₄ concentrations (0.619, 3.902, 7.741, 15.483, 31.585, and

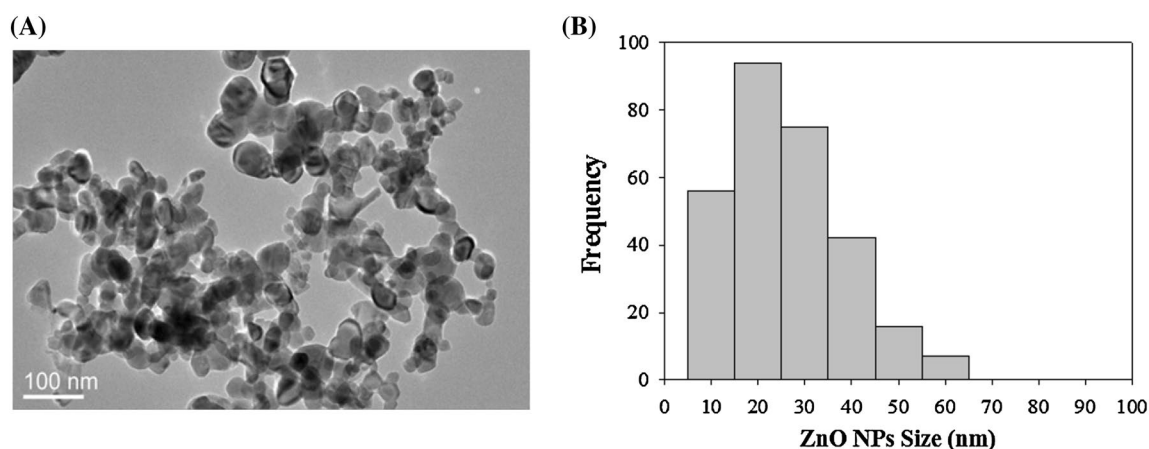


Fig. 1 **a** Transmission electron microscopy image showing the morphologies of the ZnO nanoparticles and **b** a histogram of the ZnO nanoparticle (NP) size distribution

Table 1 Characteristics of the ZnO nanoparticles and the dissolved Zn concentrations in the suspensions and solutions used in the experiments

		Dissolved Zn conc. ($\mu\text{mol/L}$)		Hydrodynamic diameter of the nanoparticles (nm) ^a		Z-potential (mV) ^a	
		After 0 h	After 72 h	After 0 h	After 72 h	After 0 h	After 72 h
		ZnO nanoparticles (10–30 nm)	LC ₁₀ (1.032 $\mu\text{mol/L}$)	0.06	0.10	291.40	NA
	LC ₃₀ (3.955 $\mu\text{mol/L}$)	0.49	0.55	691.60	NA	21.46	27.00
ZnSO ₄	LC ₁₀ (29.838 $\mu\text{mol/L}$)	10.46	9.40	– ^b	– ^b	– ^b	– ^b
	LC ₃₀ (38.422 $\mu\text{mol/L}$)	13.35	13.38	– ^b	– ^b	– ^b	– ^b

^aThe hydrodynamic diameters and zeta-potentials were determined by dynamic light scattering when the suspensions were prepared (0 h) and after the suspensions had been left for 72 h

^bNot applicable; NA, not available

619.310 $\mu\text{mol/L}$). The LC₁₀ and LC₃₀ values for the ZnO NPs and ZnSO₄ were determined using a linear regression method (CETIS v1.8.7; Tidepool, McKinleyville, CA, USA). For the microarray analyses, zebrafish larvae at 72 hpf were exposed to ZnO NPs for 72 h. An aliquot of the ZnO NP suspension was added to the zebrafish culture water in each beaker to give the control concentration or a nominal concentration of 1.032 $\mu\text{mol/L}$ (the LC₁₀) or 3.955 $\mu\text{mol/L}$ (the LC₃₀). Reference treatments using ZnSO₄ at concentrations of 29.838 $\mu\text{mol/L}$ (the LC₁₀) and 38.422 $\mu\text{mol/L}$ (the LC₃₀) were also performed to allow the toxic effects of the ZnO NPs to be compared with the toxic effects of zinc ions. Each treatment was performed in triplicate. After the larvae had been exposed to ZnO NPs or ZnSO₄ for 72 h, they were anesthetized using tricaine methanesulfonate (MS-222; Sigma-Aldrich, St. Louis, MO, USA) at a concentration of 100 mg/L following guidelines provided by the Institutional Animal Care and Use Committee of the Korea Institute of Toxicology.

The total RNA isolated from ~70 individual zebrafish larvae cultured in the same dish was treated using an RNeasy mini kit (Qiagen, Hilden, Germany). The RNA integrity was confirmed by checking the RNA integrity number using an Agilent Bioanalyzer 2100 and an Agilent RNA 6000 Nano Kit (Agilent Technologies, Wilmington, DE, USA).

One-color microarray analyses to determine gene expression in the zebrafish larvae were performed using a NEX BiO system (Daejeon, Korea) using an Agilent zebrafish oligo microarray (4×44 K; Agilent Technologies) containing 43,803 zebrafish probes. Three replicates were independently collected for each treatment, and a total of 15 microarray assays were conducted. The steps between RNA labeling and scanning were performed following the “one-color microarray-based gene expression analysis (low input quick amp labeling)” protocol provided by Agilent Technologies with slight modifications.

The total RNA was amplified using a Low RNA Input Linear Amplification kit (Agilent Technologies) and labeled using 1.65 μg of Cyanine three following the manufacturer’s instructions. Labeled cRNA was purified using an RNeasy mini kit (Qiagen). Each slide was hybridized with cRNA labeled with Cyanine three using a Gene Expression Hybridization kit (Agilent Technologies) for 17 h, then each slide was washed with the stabilization and drying solution provided in a Gene Expression Wash Buffer kit (Agilent Technologies). The microarray slides were scanned using an Agilent Scanner B system (Agilent Technologies), and the signal intensities were analyzed using Feature Extraction 10.7 software (Agilent Technologies) using the default settings. The raw data were normalized using the percentile shift method.

Each microarray dataset was analyzed using the significance analysis of microarrays method described by Tusher et al. (2001). Genes that showed significant expression changes (by a factor of more than two) were selected with a q value cutoff of 5%. The genes were classified by performing gene set enrichment analysis, which assigned genes for which significant differences were found in the ZnO NP and ZnSO₄ treatments to previously defined pathways. The gene set enrichment analysis results were analyzed using Ingenuity Pathway Analysis software (Ingenuity Systems, Redwood City, CA, USA).

Results and Discussion

The estimated 72 h LC₁₀ and LC₃₀ values for the ZnO NPs for zebrafish larvae at 72 hpf were 1.032 and 3.955 $\mu\text{mol/L}$, respectively, and the estimated 72 h LC₁₀ and LC₃₀ values for ZnSO₄ for zebrafish larvae at 72 hpf were 29.838 and 38.422 $\mu\text{mol/L}$, respectively. This indicated that the ZnO NPs were markedly more toxic than ZnSO₄ to the larval zebrafish. Differently expressed genes (DEGs) were

identified from the microarray-based expression dataset, and these DEGs allowed the responses to the ZnO NPs and the cytotoxicities of the ZnO NPs to be predicted. As is shown in Fig. 2, marked transcriptional responses to exposure to ZnO NPs relative to the controls were not found, but a number of genes were upregulated or downregulated in zebrafish exposed to ZnSO₄ relative to the controls.

These results suggest that the ZnO NPs were more toxic than ZnSO₄ but that the ZnO NPs did not cause significant gene expression changes relative to the controls, indicating that the physical properties of the ZnO NPs may have been responsible for the increased zebrafish larvae mortality. It has previously been found that increased mortality in fish larvae exposed to ZnO NPs was related to mouth-gaping behavior leading to increased uptake of the ZnO NPs (Zhou et al. 2015). Lin et al. (2013) found that hatched larvae take up NPs through the gills, intestines, skin, and other organs, and that, therefore, toxicological responses to NP exposure may be related to the sizes of NPs. It has been found that zebrafish mortality was more markedly increased by exposure to ZnO NPs than by bulk ZnO (Xiong et al. 2011), which could indicate that the particle size could be the most important factor controlling ZnO NP toxicity to hatched larvae (when each larva was not protected by the chorion). It has been suggested that the release of zinc ions plays an important role in the effects of ZnO NPs on gene expression (Shen et al. 2013), but we found that relatively small amounts of zinc ions were released at the ZnO NP LC₁₀ and LC₃₀. We found a negative correlation between gene expression changes and ZnO NP toxicity to the zebrafish larvae. In contrast, it has previously been found that the

number of significantly altered transcripts increased dose-dependently as the ZnSO₄ concentration increased, suggesting that an overload of cellular zinc ions can activate or inhibit molecular mechanisms by interfering with zinc ion homeostasis (Kao et al. 2012).

As is shown in Fig. 2, the number of upregulated DEGs at the ZnSO₄ LC₁₀ relative to the controls and at the ZnSO₄ LC₁₀ relative to the ZnO NP LC₁₀ were similar, indicating that the ZnO NPs at the LC₁₀ did not affect the number of upregulated DEGs. However, the proportion of DEGs that were upregulated decreased when the ZnSO₄ LC₃₀ results were compared with the ZnO NP LC₃₀ results rather than the control results, indicating that more than half of the upregulated DEGs at the ZnSO₄ LC₃₀ relative to the controls were also activated by the ZnO NPs at the LC₃₀. We analyzed the canonical pathways of the upregulated DEGs at the ZnSO₄ LC₃₀ using ingenuity pathway analysis. As is shown in Fig. 3a, b the ranked pathway order and ratio values were different, suggesting that different pathways were affected at the ZnO NP LC₃₀. In particular, the pathways affected at the ZnO NP LC₃₀ were associated with cell differentiation and the immune system. It has been found in recent studies that ZnO NPs induce 3T3-L1 adipocyte differentiation in mouse embryos and inflammatory responses (such as the release of pro-inflammatory cytokines) in both mammalian cells and zebrafish (Brun et al. 2014; Saptarshi et al. 2015; Pandurangan et al. 2016).

As is shown in Fig. 2, twice as many DEGs were downregulated at the ZnSO₄ LC₁₀ relative to at the ZnO NP LC₁₀ than at the ZnSO₄ LC₁₀ relative to the controls, indicating that some of the DEGs that were downregulated at the

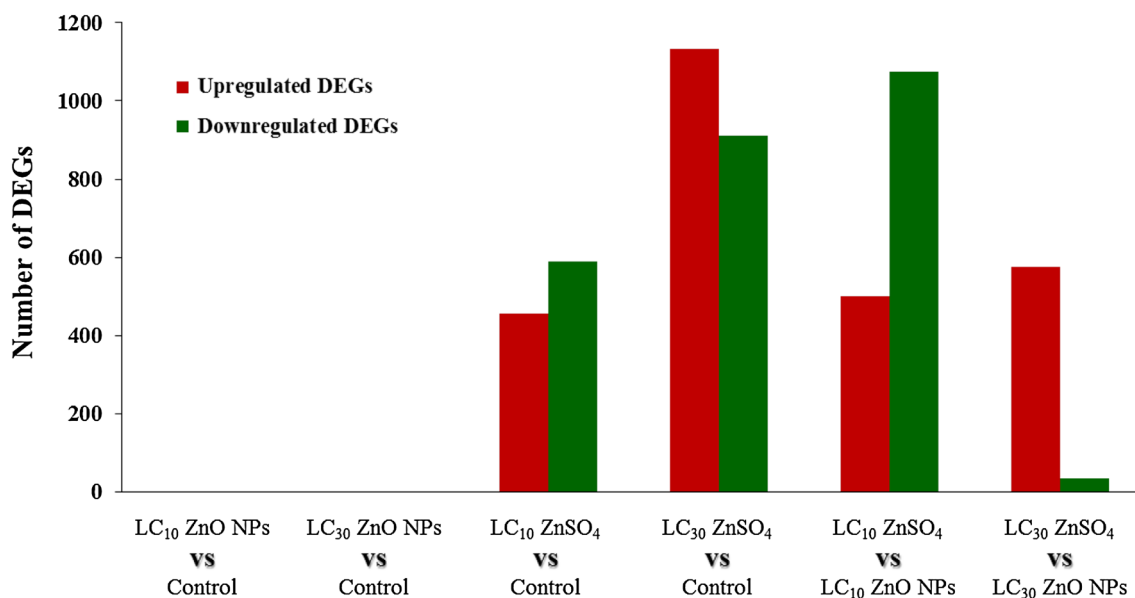
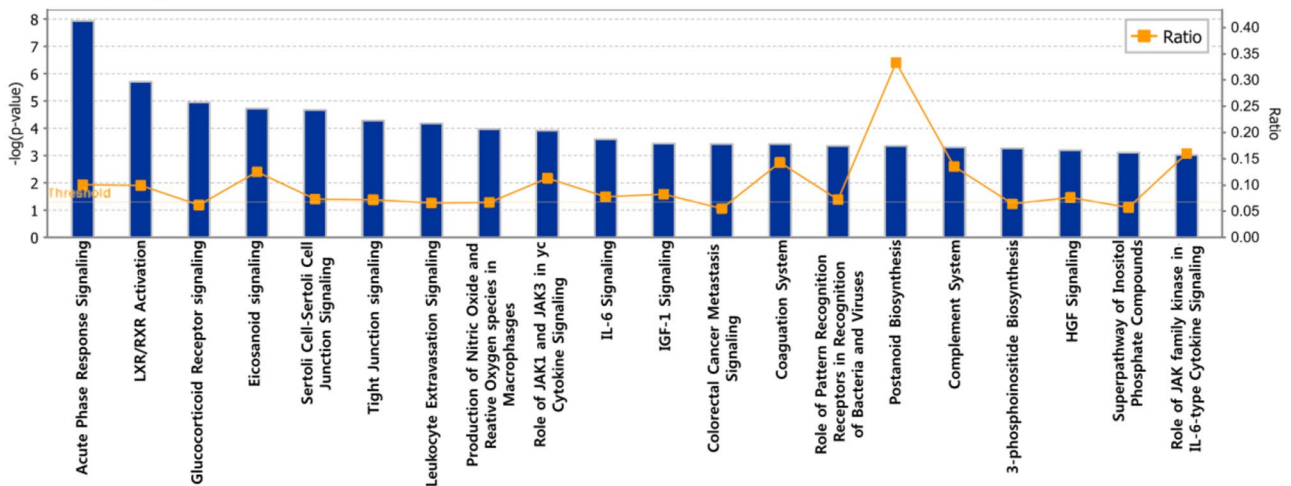


Fig. 2 Numbers of differently expressed genes (DEGs) in zebrafish exposed to different concentrations (the LC₁₀ and LC₃₀) of ZnO nanoparticles (NPs) and ZnSO₄ relative to the three groups (control, LC₁₀ ZnO NPs, and LC₃₀ ZnO NPs)

(A) ZnSO₄ LC₃₀ VS Control



(B) ZnSO₄ LC₃₀ VS ZnO NPs LC₃₀

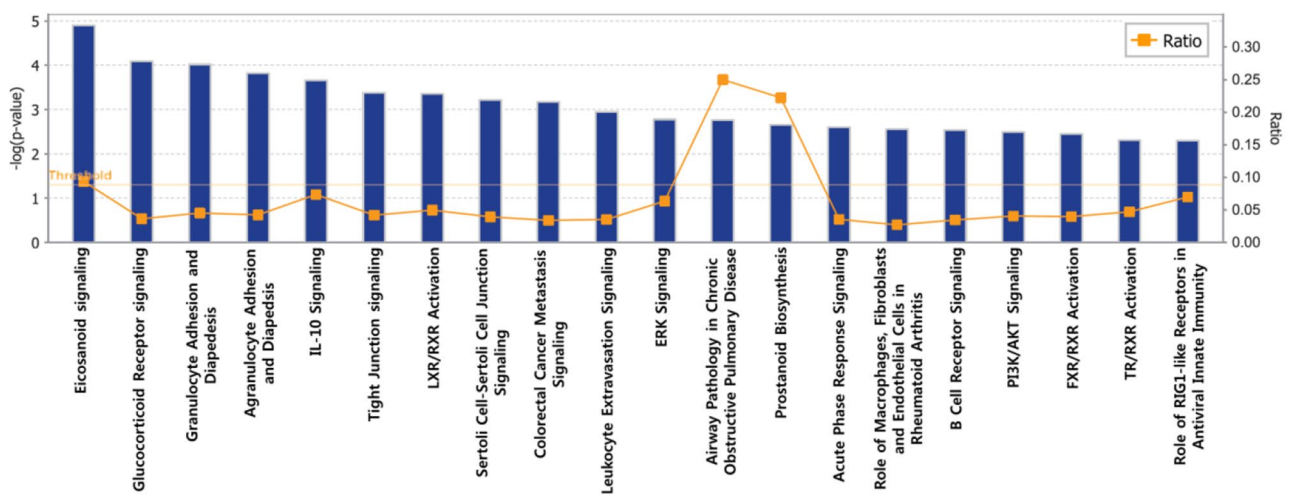


Fig. 3 Canonical pathway analysis results obtained using ingenuity pathway analysis for upregulated differently expressed genes in response to exposure to **a** ZnSO₄ at the LC₃₀ relative to the control and **b** ZnSO₄ at the LC₃₀ relative to exposure to ZnO NPs. The bars measured against the Y-axis on the left, are the negative logarithms

of the *p*-values. The threshold was a $-\log(p\text{-value})$ value of 1.3 (corresponding to a *p*-value of 0.05). The square markers and line, measured against the Y-axis on the right, are the gene number ratios for the pathways that met the cutoff criteria.

ZnSO₄ LC₁₀ relative to at the ZnO NP LC₁₀ were upregulated at the ZnO NP LC₁₀. As is shown in Table 2, the canonical pathways that were identified for the DEGs that were downregulated at the ZnSO₄ LC₁₀ relative to at the ZnO NP LC₁₀ were typically related to cancer cell differentiation, endocytic transport, and genes such as the epidermal growth factor receptor (EGFR), V-Ki-ras2 Kirsten rat sarcoma viral oncogene homolog (KRAS), and phosphoinositide-3-kinase regulatory subunit 6 (PIK3R6) genes.

KRAS and EGFR are important effector genes in tumorigenesis and tumor progress, and PIK3R6 also plays an oncogenic role in several cancers (Markman et al.

2010; Zhou et al. 2012). In particular, mutated *kras* and *egfr* genes are the most powerful predictors in several cancer cell lines (Suda et al. 2010; Misale et al. 2012). With regard to NP toxicity, Shvedova et al. (2014) found that single-walled carbon nanotubes and carbon nanofibers increase the incidence of KRAS oncogene mutations in the lung. The genotoxicities of nanotubes have been demonstrated by the presence of cellular defects, such as chromosomal aberrations, enhanced micronuclei frequencies, and increased DNA strands in cells exposed to nanotubes (Schins et al. 2012). The activation of the *kras* and *egfr* genes induced by the exposure of larval zebrafish to

Table 2 The top five canonical pathways results obtained using ingenuity pathway analysis for downregulated differently expressed genes at the ZnSO₄ LC₁₀ relative to the ZnO NP LC₁₀

Ingeniuty canonical pathway	<i>p</i> -value	Genes
Caveolar-mediated endocytosis signaling	2.10 × 10 ⁻⁴	ITGAM, EGFR, HLA-A, DNM2, PTRF, ITGB8, HLA-B
Estrogen-dependent breast cancer signaling	7.20 × 10 ⁻⁴	KRAS, EGFR, PIK3R6, HSD17B1, TERT, ESR1
Bladder cancer signaling	7.33 × 10 ⁻⁴	KRAS, EGFR, ERBB2, FGF8, FGF23, MMP13, PDGFC
Endothelial nitric oxide synthase signaling	7.73 × 10 ⁻⁴	CCNA1, PIK3R6, DNM2, NOSTRIN, GUCY1A3, CNGA2, ADCY8, ESR1, PDGFC
Virus entry via endocytic pathways	8.39 × 10 ⁻⁴	KRAS, HLA-A, PIK3R6, DNM2, AP2A1, ITGB8, HLA-B

ZnO NPs at the LC₁₀ may therefore indicate that ZnO NP toxicity can potentially lead to genotoxic effects. Sharma et al. (2009) found that ZnO NPs at low concentrations can be genotoxic to human epidermal cells. However, further studies will need to be performed to determine whether the induction of *kras* and *egfr* gene expression is closely linked to the pathways associated with ZnO NP toxicity and the downstream effects of ZnO NP toxicity. Unlike results found previously, most of the DEGs that were downregulated at the ZnSO₄ LC₃₀ relative to the controls were not downregulated at the ZnSO₄ LC₃₀ relative to at the ZnO NP LC₃₀, indicating that the ZnO NPs and ZnSO₄ at their LC₃₀s inactivated similar biological processes, such as cholesterol synthesis and the cell cycle (data not shown).

In conclusion, we found that ZnO NPs are relatively toxic to larval zebrafish even though they do not, compared with ZnSO₄, markedly modulate transcripts. The different DEG patterns for the ZnO NPs and ZnSO₄ might be caused by the physical properties of the NPs rather than the release of zinc ions from the ZnO NPs, implying that ZnO NPs and ZnSO₄ have different toxic mechanisms. Comparison analysis of the microarray data using ingenuity pathway analysis showed that the inflammation system and several genes involved in cancer cell differentiation were altered in zebrafish larvae exposed to ZnO NPs. The genes that were activated by exposure to ZnO NPs were not affected to a significant degree (the number of fold changes was not greater than two), but our results provide clues that will help in the interpretation of the molecular mechanisms that underlie changes in the gene expression regulatory networks caused by exposure to ZnO NPs. Further studies will be required to elucidate the relationships between the uptake kinetics of unequally sized or shaped ZnO NPs and cellular pathology.

Acknowledgements This study was supported through grants KK-1608 and KK-1610-04 provided by the Korea Institute of Toxicology (KIT, Korea).

References

- Aitken RJ, Chaudhry MQ, Boxall ABA, Hull M (2006) Manufacture and use of nanomaterials: current status in the UK and global trends. *Occup Med* 56:300–306
- Berry JP, Gantar M, Gibbs PDL, Schmale MC (2007) The zebrafish (*Danio rerio*) embryo as a model system for identification and characterization of developmental toxins from marine and freshwater microalgae. *Comp Biochem Physiol* 145:61–72.
- Bondarenko O, Juganson K, Ivask A, Kasemets K, Mortimer M, Kahru A (2013) Toxicity of Ag, CuO and ZnO nanoparticles to selected environmentally relevant test organisms and mammalian cells in vitro: a critical review. *Arch Toxicol* 87:1181–1200
- Brun NR, Lenz M, Wehrli B, Fent K (2014) Comparative effects of zinc oxide nanoparticles and dissolved zinc on zebrafish embryos and eleuthero-embryos: importance of zinc ions. *Sci Total Environ* 476:657–666
- Bystrzejewska-Piotrowska G, Golimowski J, Urban PL (2009) Nanoparticles: their potential toxicity, waste and environmental management. *Waste Manage* 29:2587–2595
- Chen TH, Lin CC, Meng PJ (2014) Zinc oxide nanoparticles alter hatching and larval locomotor activity in zebrafish (*Danio rerio*). *J Hazard Mater* 277:134–140
- El Badawy AM, Silva RG, Morris B, Scheckel KG, Suidan MT, Tolaymat TM (2010) Surface charge-dependent toxicity of silver nanoparticles. *Environ Sci Technol* 45:283–287
- Felix LC, Ortega VA, Ede JD, Goss GG (2013) Physicochemical characteristics of polymer-coated metal-oxide nanoparticles and their toxicological effects on zebrafish (*Danio rerio*) development. *Environ Sci Technol* 47:6589–6596
- Fukui H, Horie M, Endoh S, Kato H, Fujita K, Nishio K, Komaba LK, Maru J, Miyauhi A, Kinugasa S, Yoshida Y, Hagihara Y, Iwahashi H (2012) Association of zinc ion release and oxidative stress induced by intratracheal instillation of ZnO nanoparticles to rat lung. *Chem-Biol Interact* 198:29–37
- Gilbert B, Fakra SC, Xia T, Pokhrel S, Mädler L, Nel AE (2012) The fate of ZnO nanoparticles administered to human bronchial epithelial cells. *ACS Nano* 6:4921–4930
- Gottschalk F, Sonderer T, Scholz RW, Nowack B (2009) Modeled environmental concentrations of engineered nanomaterials (TiO₂, ZnO, Ag, CNT, fullerenes) for different regions. *Environ Sci Technol* 43:9216–9222
- Gottschalk F, Sonderer T, Scholz RW, Nowack B (2010) Possibility and limitations of modeling environmental exposure to engineered nanomaterials by probabilistic material flow analysis. *Environ Toxicol Chem* 29:1036–1048

- Griffitt RJ, Lavelle CM, Kane AS, Denslow ND, Barber DS (2013) Chronic nanoparticulate silver exposure results in tissue accumulation and transcriptomic changes in zebrafish. *Aquat Toxicol* 130–131:192–200
- Hill AJ, Howard CV, Cossins AR (2002) Efficient embedding technique for preparing small specimens for stereological volume estimation: Zebrafish larvae. *J Microsc* 206:179–181
- Jiang J, Oberdörster G, Elder A, Gelein R, Mercer P, Biswas P (2008) Does nanoparticle activity depend upon size and crystal phase?. *Nanotoxicology* 2:33–42
- Kao YY, Chen YC, Cheng TJ, Chiung YM, Liu PS (2012) Zinc oxide nanoparticles interfere with zinc ion homeostasis to cause cytotoxicity. *Toxicol Sci* 125:462–472
- Lee JH, Ju JE, Kim BI, Pak PJ, Choi EK, Lee HS, Chung N (2014) Rod-shaped iron oxide nanoparticles are more toxic than sphere-shaped nanoparticles to murine macrophage cells. *Environ Toxicol Chem* 33:2759–2766
- Lin S, Zhao Y, Nel AE, Lin S (2013) Zebrafish: an in vivo model for nano EHS studies. *Small* 9:1608–1618
- Long Y, Li L, Li Q, He X, Cui Z (2012) Transcriptomic characterization of temperature stress responses in larval zebrafish. *PLoS ONE* 7:e37209.
- Markman B, Ramos FJ, Capdevila J, Taberero J (2010) EGFR and KRAS in colorectal cancer. *Adv Clin Chem* 51:71–119
- Misale S, Yaeger R, Hobor S, Scala E, Janakiraman M, Liska D, Valtorta E, Schiavo R, Buscarino M, Siravegna G, Bencardino K, Cercek A, Chen CT, Veronese S, Zanon C, Sartore-Bianchi A, Gambacorta M, Gallicchio M, Vakiani E, Boscaro V, Medico E, Weiser M, Siena S, Di Nicolantonio F, Solit D, Bardelli A (2012) Emergence of KRAS mutations and acquired resistance to anti-EGFR therapy in colorectal cancer. *Nature* 486:532–536
- Pandurangan M, Jin BY, Kim DH (2016) ZnO Nanoparticles upregulate adipocyte differentiation in 3T3-L1 cells. *Biol Trace Elem Res* 170:201–207
- Saptarshi SR, Feltis BN, Wright PFA, Lopata AL (2015) Investigating the immunomodulatory nature of zinc oxide nanoparticles at sub-cytotoxic levels in vitro and after intranasal instillation in vivo. *J Nanobiotechnol* 13:6
- Schins RPF, Albrecht C, Gerloff K, van Berlo D (2012) Genotoxicity investigations with carbon nanotubes. In: Donaldson K, Poland CA, Duffin R, Bonner J (eds) *The toxicology of carbon nanotubes*. Cambridge University Press, New York, pp 153–160
- Sharma V, Shukla RK, Saxena N, Parmar D, Das M, Dhawan A (2009) DNA damaging potential of zinc oxide nanoparticles in human epidermal cells. *Toxicol Lett* 185:211–218
- Shen C, James SA, de Jonge MD, Turney TW, Wright PFA, Feltis BN (2013) Relating cytotoxicity, zinc ions, and reactive oxygen in ZnO nanoparticle-exposed human immune cells. *Toxicol Sci* 136:120–130
- Shvedova AA, Yanamala N, Kisin ER, Tkach AV, Murray AR, Hubbs A, Chirila MM, Keohavong P, Sycheva LP, Kagan VE, Castranova V (2014) Long-term effects of carbon containing engineered nanomaterials and asbestos in the lung: one year post-exposure comparisons. *Am J Physiol* 306:L170–L182
- Suda K, Tomizawa K, Mitsudomi T (2010) Biological and clinical significance of KRAS mutations in lung cancer: an oncogenic driver that contrasts with EGFR mutation. *Cancer Metastasis Rev* 29:49–60
- Tusher VG, Tibshirani R, Chu G (2001) Significance analysis of microarrays applied to the ionizing radiation response. *Proc Natl Acad Sci* 98:5116–5121
- Ung CY, Lam SH, Hlaing MM, Winata CL, Korzh S, Mathavan S, Gong Z (2010) Mercury-induced hepatotoxicity in zebrafish: in vivo mechanistic insights from transcriptome analysis, phenotype anchoring and targeted gene expression validation. *BMC Genom* 11(1):212
- Westerfield M (1995) *The zebrafish book: a guide for the laboratory use of zebrafish (Brachydanio rerio)*. University of Oregon Press, Eugene
- Xia T, Zhao Y, Sager T, George S, Pokhrel S, Li N, Li N, Schoenfeld D, Meng H, Lin S, Wang X, Wang M, Ji Z, Zink JJ, Madler L, Castranova V, Lin S, Nel AE (2011) Decreased dissolution of ZnO by iron doping yields nanoparticles with reduced toxicity in the rodent lung and zebrafish embryos. *ACS Nano* 5:1223–1235
- Xiong D, Fang T, Yu L, Sima X, Zhu W (2011) Effects of nano-scale TiO₂, ZnO and their bulk counterparts on zebrafish: Acute toxicity, oxidative stress and oxidative damage. *Sci Total Environ* 409:1444–1452
- Zhao X, Wang S, Wu Y, You H, Lv L (2013) Acute ZnO nanoparticles exposure induces developmental toxicity, oxidative stress and DNA damage in embryo-larval zebrafish. *Aquat Toxicol* 136–137:49–59
- Zhou J, Chen GB, Tang YC, Sinha RA, Wu Y, Yap CS, Wang G, Hu J, Xia X, Tan P, Goh LK, Yen PM (2012) Genetic and bioinformatic analyses of the expression and function of PI3K regulatory subunit PIK3R3 in an Asian patient gastric cancer library. *BMC Med Genomics* 5:34
- Zhou Z, Son J, Harper B, Zhou Z, Harper S (2015) Influence of surface chemical properties on the toxicity of engineered zinc oxide nanoparticles to embryonic zebrafish. *Beilstein J Nanotechnol* 20:1568–1579